

An Iterative CN-Leapfrog Scheme Based Hybrid Implicit–Explicit Discontinuous Galerkin Finite-Element Time-Domain Method for Analysis of Multiscale Problems

M. Li^{1,2}, X. D. Ye³, F. Xu¹, and Y. T. Yang³

¹ School of Electronic Science and Engineering
Nanjing University of Posts and Telecommunications, Nanjing, 210003, China

² Department of Electronic Information Engineering
Suqian College, Suqian, 223800, China
18800608557@163.com

³ Department of Communication Engineering
Nanjing University of Science and Technology, Nanjing, 210094, China
yexiaodong@njjust.edu.cn

Abstract — The discontinuous Galerkin finite-element time-domain (DG-FETD) method with the ability to deal with unstructured meshes is well suited to analyze the multiscale system. However the DG-FETD method with explicit integration schemes is constrained by stability conditions that can be very restrictive upon highly fine meshes. The hybrid implicit–explicit Crank-Nicolson (CN) leapfrog scheme is effective in solving this problem; but because of using CN scheme, the inversion of a large sparse matrix must be calculated at each time step in the fine regions. The hybrid implicit–explicit iterative CN leapfrog scheme is introduced to improve the computational efficiency which can form a block diagonal matrix. The leapfrog scheme is employed for electrically coarse regions and iterative CN scheme for electrically fine ones. The numerical examples have demonstrated the validity and efficiency of the method.

Index Terms — Crank-Nicolson, discontinuous Galerkin finite-element time-domain method, multi-scale.

I. INTRODUCTION

When handling the multiscale electromagnetic simulations in transient electromagnetic analysis, such as electromagnetic interference and electromagnetic compatibility problems, traditional methods face great challenges because of small size meshes in the fine regions. The finite-element time-domain (FETD) method is widely used because of its flexibility in geometric modeling, but it must calculate a large sparse matrix inversion at each time step [1]. Then the discontinuous Galerkin method has been proposed and combined with the FETD method called discontinuous Galerkin

finite-element time-domain (DG-FETD) method [2]-[4]; Numerical fluxes are introduced to impose the tangential continuity of the electrical and magnetic fields at the interfaces between adjacent elements. Central flux [5, 6] and upwind flux [7, 8] are the commonly used ways. The explicit leapfrog scheme for DG-FETD method can make the mass matrix block-diagonal and it is convenient for matrix inversion and parallel computing rather than solve a huge matrix system as conventional FETD method [9-12]. But the size of the time step of the explicit leapfrog DG-FETD is limited by the spatial discretization of the simulation domain according to the CFL condition which will lead to produce a large number of simulation steps and reduce the computation efficiency. Generally, a discretized multiscale system usually contains both electrically coarse meshes and fine meshes. Because of the constraint of Courant-Friedrichs-Levy (CFL) stability condition [13], the time step increments for electrically fine meshes may be much less than those for electrically coarse meshes when the explicit leapfrog time integration scheme is employed. According to this circumstance, hybrid implicit-explicit Crank-Nicolson (CN) leapfrog scheme have been proposed to get a higher computational efficiency [14]. The implicit CN scheme used in fine regions can make the system unconditionally stable but also require solving large matrices equations which will destroy the original powerful ability of DG-FETD. Therefore, an iterative CN leapfrog scheme DG-FETD is proposed, which can not only make system unconditionally stable but also maintain the advantage of DG-FETD.

In this paper, an iterative CN leapfrog scheme is introduced to analyze multiscale electromagnetic

problems. The leapfrog scheme is employed for electrically coarse regions and iterative Crank-Nicholson scheme [15] for electrically fine ones. In the paper, an iterative CN leapfrog scheme is first introduced with poor convergence. To solve the poor convergence problem, a modified iterative CN leapfrog scheme is further presented to speed up the convergence.

The paper is organized as follows. The basic theory and formulations of the hybrid implicit–explicit iterative CN leapfrog scheme for DG-FETD is presented in Section II. The numerical results are given to demonstrate the validity of proposed method in Section III, and the conclusion is drawn in Section IV.

II. THEORY AND FORMULATIONS

A. DG-FETD spatial semi-discrete formulation

The implementation steps of the DG-FETD method include choice of the governing equation, grid discretization and imposing the tangential continuity of the electrical and magnetic fields at the interfaces between adjacent elements. In this paper, first order Maxwell's curl equations based on \mathbf{E} and \mathbf{H} are employed and the model is discretized by tetrahedral meshes, central flux scheme is employed. Considering the time-dependent Maxwell's curl equations for a linear, lossless, isotropic and non-dispersive medium, the electric field \mathbf{E} and the magnetic field \mathbf{H} can be described as:

$$\varepsilon \frac{\partial \mathbf{E}}{\partial t} = \nabla \times \mathbf{H}, \quad (1)$$

$$\mu \frac{\partial \mathbf{H}}{\partial t} = -\nabla \times \mathbf{E}, \quad (2)$$

where ε represents the permittivity and μ denotes the permeability. The electric and magnetic fields can be expanded by Whitney edge elements [16] as:

$$\mathbf{E} = \sum_j \mathbf{W}_{ej} e_j, \quad \mathbf{H} = \sum_j \mathbf{W}_{hj} h_j. \quad (3)$$

The curl-conforming vector basis functions \mathbf{W}_{ej} and \mathbf{W}_{hj} are chosen to discretize the \mathbf{E} field and \mathbf{H} field respectively. Then e_j and h_j are the unknown coefficients. The Galerkin's weak forms of Maxwell's equations can be described as:

$$\iiint_V \mathbf{W}_{ei} \cdot \varepsilon \frac{\partial \mathbf{E}}{\partial t} dV - \iiint_V \nabla \times \mathbf{W}_{ei} \cdot \mathbf{H} dV = \iint_S \mathbf{W}_{ei} \cdot (\mathbf{n} \times \mathbf{H}) dS, \quad (4)$$

$$\iiint_V \mathbf{W}_{hi} \cdot \mu \frac{\partial \mathbf{H}}{\partial t} dV + \iiint_V \nabla \times \mathbf{W}_{hi} \cdot \mathbf{E} dV = \iint_S \mathbf{W}_{hi} \cdot (\mathbf{n} \times \mathbf{E}) dS. \quad (5)$$

The central flux is employed for each element to impose the tangential continuity of the electric and magnetic fields at the interfaces between adjacent elements and the expression is:

$$\mathbf{n} \times \mathbf{H} \Big|_{\partial V} = \frac{1}{2} \mathbf{n} \times (\mathbf{H} + \mathbf{H}^+) \Big|_{\partial V}, \quad (6)$$

$$\mathbf{n} \times \mathbf{E} \Big|_{\partial V} = \frac{1}{2} \mathbf{n} \times (\mathbf{E} + \mathbf{E}^+) \Big|_{\partial V}, \quad (7)$$

where \mathbf{E} and \mathbf{H} represent the electric and magnetic fields of the elements within sub-domain V , \mathbf{E}^+ and \mathbf{H}^+ represent electric and magnetic fields of the adjacent elements within the neighboring sub-domain V^+ . By substituting (6) and (7) into (4) and (5), the final spatial semi-discrete DG-FETD formulations can be converted into a matrix equation as follows:

$$\mathbf{T}_{ee} \frac{\partial \mathbf{e}}{\partial t} = \mathbf{P}_{eh} \mathbf{h} + \mathbf{S}_{eh}^+ \mathbf{h}, \quad (8),$$

$$\mathbf{T}_{hh} \frac{\partial \mathbf{h}}{\partial t} = \mathbf{P}_{he} \mathbf{e} + \mathbf{S}_{he}^+ \mathbf{e}, \quad (9)$$

where \mathbf{T}_{ee} , \mathbf{T}_{hh} , \mathbf{P}_{eh} , \mathbf{P}_{he} , \mathbf{S}_{eh}^+ and \mathbf{S}_{he}^+ are the sparse matrices, \mathbf{e} and \mathbf{h} are the unknown vectors. The matrix elements are defined as:

$$[\mathbf{T}_{ee}]_{ij} = \varepsilon \iiint_V \mathbf{W}_{ei} \cdot \mathbf{W}_{ej} dV,$$

$$[\mathbf{T}_{hh}]_{ij} = \mu \iiint_V \mathbf{W}_{hi} \cdot \mathbf{W}_{hj} dV,$$

$$[\mathbf{P}_{eh}]_{ij} = \iiint_V \nabla \times \mathbf{W}_{ei} \cdot \mathbf{W}_{hj} dV + \frac{1}{2} \iint_S \mathbf{W}_{ei} \cdot \mathbf{n} \times \mathbf{W}_{hj} dS,$$

$$[\mathbf{P}_{he}]_{ij} = -\iiint_V \nabla \times \mathbf{W}_{hi} \cdot \mathbf{W}_{ej} dV - \frac{1}{2} \iint_S \mathbf{W}_{hi} \cdot \mathbf{n} \times \mathbf{W}_{ej} dS,$$

$$[\mathbf{S}_{eh}^+]_{ij} = \frac{1}{2} \iint_S \mathbf{W}_{ei} \cdot \mathbf{n} \times \mathbf{W}_{hj}^+ dS,$$

$$[\mathbf{S}_{he}^+]_{ij} = -\frac{1}{2} \iint_S \mathbf{W}_{hi} \cdot \mathbf{n} \times \mathbf{W}_{ej}^+ dS.$$

B. Iterative CN-leapfrog scheme

When dealing with multiscale electromagnetic problems, very small size meshes will appear in fine regions of the model. Though explicit leapfrog scheme of the DG-FETD method makes the mass matrix block-diagonal and it is convenient for matrix inversion and parallel computing. But the size of the time step of the explicit leapfrog DG-FETD is limited by the spatial discretization of the simulation domain according to the CFL condition which lead to produce a large number of simulation steps and reduce the computation efficiency. In contrast, the implicit time step schemes are proved to be unconditionally stable with large time step intervals but require solving large matrix equations. Therefore, hybrid implicit-explicit CN leapfrog scheme can be attractive in multi-scale electromagnetic simulations. However, the implicit-explicit CN leapfrog DG-FETD lost the block diagonal characteristic because of using implicit CN scheme which lead to a mass matrix of DG-FETD. In this section, an iterative CN Leapfrog scheme is proposed to deal with the above problems

which can not only maintain the block diagonal characteristic of the DG-FETD method but also improve the computational efficiency.

The proposed hybrid iterative CN Leapfrog scheme divides the whole computational domain into the coarse region marked by region 1 and the fine region marked by region 2, [1]. In region 1, explicit leapfrog scheme is employed to DG-FETD method and the Eq. (8), Eq. (9) above can be changed into:

$$\mathbf{T}_{hh} \frac{h^{n+\frac{1}{2}} - h^{n-\frac{1}{2}}}{\Delta t} = \mathbf{P}_{he} e^n + \frac{1}{2} (\mathbf{S}_{he} e^n + \mathbf{S}_{he}^+ e^n), \quad (10)$$

$$\mathbf{T}_{ee} \frac{e^{n+1} - e^n}{\Delta t} = \mathbf{P}_{eh} h^{n+\frac{1}{2}} + \frac{1}{2} (\mathbf{S}_{eh} h^{n+\frac{1}{2}} + \mathbf{S}_{eh}^+ h^{n+\frac{1}{2}}). \quad (11)$$

Where Δt represents the time step size and can be expressed as:

$$\Delta t \leq \frac{h_{\min}}{2v_{\max}(p+1)^2},$$

where h_{\min} is the minimum length of the mesh, v_{\max} is the propagation speed of the wave in the object, p is the order of the base function.

In region 2, iterative CN scheme is applied to DG-FETD method and the Eq. (8), Eq. (9) can be expressed as:

$$\mathbf{T}_{hh} \frac{h^{n+1} - h^n}{\Delta t} = \mathbf{P}_{he} \cdot \frac{e^{n+1} + e^n}{2} + \mathbf{S}_{he} \cdot \frac{e^{n+1} + e^n}{2} + \mathbf{S}_{he}^+ \cdot \frac{e^{n+1} + e^n}{2}, \quad (12)$$

$$\mathbf{T}_{ee} \frac{e^{n+1} - e^n}{\Delta t} = \mathbf{P}_{eh} \cdot \frac{h^{n+1} + h^n}{2} + \mathbf{S}_{eh} \cdot \frac{h^{n+1} + h^n}{2} + \mathbf{S}_{eh}^+ \cdot \frac{h^{n+1} + h^n}{2}. \quad (13)$$

The proposed scheme can be described by the following steps:

Step 1. Assume that the correct overall distribution of the electromagnetic fields at the time of $n\Delta t$ is known.

Step 2. In region 1, the leapfrog scheme for DG-FETD as Eq. (10) and Eq. (11) calculate the electric and magnetic fields at the time of $(n + \frac{1}{2})\Delta t$:

$$\begin{cases} \mathbf{T}_{hh1} \cdot \frac{h_1^{n+\frac{1}{2}} - h_1^n}{\Delta t / 2} = \mathbf{P}_{he1} \cdot e_1^n + \mathbf{S}_{he1} \cdot e_1^n + \mathbf{S}_{he1}^+ \cdot e_1^n + \mathbf{S}_{he12}^+ \cdot e_2^n \\ \mathbf{T}_{ee1} \cdot \frac{e_1^{n+\frac{1}{2}} - e_1^n}{\Delta t / 2} = \mathbf{P}_{eh1} \cdot h_1^{n+\frac{1}{2}} + \mathbf{S}_{eh1} \cdot h_1^{n+\frac{1}{2}} + \mathbf{S}_{eh1}^+ \cdot h_1^{n+\frac{1}{2}} + \mathbf{S}_{eh12}^+ \cdot h_2^n \end{cases}. \quad (14)$$

Step 3. In region 2, CN scheme for DG-FETD as Eq. (12) and Eq. (13) calculate the electric and magnetic fields at the time of $(n+1)\Delta t$:

$$\begin{cases} \mathbf{T}_{hh2} \cdot \frac{h_2^{n+1} - h_2^n}{\Delta t} \\ = \mathbf{P}_{he2} \cdot \frac{e_2^{n+1} + e_2^n}{2} + \mathbf{S}_{he2} \cdot \frac{e_2^{n+1} + e_2^n}{2} + \mathbf{S}_{he2}^+ \cdot \frac{e_2^{n+1} + e_2^n}{2} + \mathbf{S}_{he21}^+ \cdot e_1^{n+\frac{1}{2}} \\ \mathbf{T}_{ee2} \cdot \frac{e_2^{n+1} - e_2^n}{\Delta t} \\ = \mathbf{P}_{eh2} \cdot \frac{h_2^{n+1} + h_2^n}{2} + \mathbf{S}_{eh2} \cdot \frac{h_2^{n+1} + h_2^n}{2} + \mathbf{S}_{eh2}^+ \cdot \frac{h_2^{n+1} + h_2^n}{2} + \mathbf{S}_{eh21}^+ \cdot h_1^{n+\frac{1}{2}} \end{cases}. \quad (15)$$

Equation (15) can be converted into a matrix equation:

$$\begin{bmatrix} \mathbf{T}_{ee2} & -\Delta t \frac{\mathbf{P}_{eh2} + \mathbf{S}_{eh2}}{2} \\ -\Delta t \frac{\mathbf{P}_{he2} + \mathbf{S}_{he2}}{2} & \mathbf{T}_{hh2} \end{bmatrix} \begin{bmatrix} e_2^{n+1} \\ h_2^{n+1} \end{bmatrix} + \mathbf{S}_{eh2}^+ \begin{bmatrix} e_2^{n+1} \\ h_2^{n+1} \end{bmatrix} + \mathbf{S}_{he2}^+ \begin{bmatrix} e_2^{n+1} \\ h_2^{n+1} \end{bmatrix} \\ = \begin{bmatrix} \mathbf{T}_{ee2} & \Delta t \frac{\mathbf{P}_{eh2} + \mathbf{S}_{eh2} + \mathbf{S}_{eh2}^+}{2} \\ \Delta t \frac{\mathbf{P}_{he2} + \mathbf{S}_{he2} + \mathbf{S}_{he2}^+}{2} & \mathbf{T}_{hh2} \end{bmatrix} \begin{bmatrix} e_2^n \\ h_2^n \end{bmatrix} \\ + \begin{bmatrix} \Delta t \mathbf{S}_{eh21}^+ \\ \Delta t \mathbf{S}_{he21}^+ \end{bmatrix} \begin{bmatrix} e_1^{n+\frac{1}{2}} \\ h_1^{n+\frac{1}{2}} \end{bmatrix}, \quad (16)$$

because \mathbf{S}_{eh2}^+ and \mathbf{S}_{he2}^+ present the matrices of the adjacent element in region 2 which destroy the block diagonal characteristic of the mass matrix, \mathbf{S}_{eh2}^+ and \mathbf{S}_{he2}^+ are moved to the right-hand side of the equation to ensure the mass matrix of the left-hand side is a block diagonal matrix:

$$\begin{bmatrix} \mathbf{T}_{ee2} & -\Delta t \frac{\mathbf{P}_{eh2} + \mathbf{S}_{eh2}}{2} \\ -\Delta t \frac{\mathbf{P}_{he2} + \mathbf{S}_{he2}}{2} & \mathbf{T}_{hh2} \end{bmatrix} \begin{bmatrix} e_2^{n+1} \\ h_2^{n+1} \end{bmatrix} \\ = \begin{bmatrix} \mathbf{T}_{ee2} & \Delta t \frac{\mathbf{P}_{eh2} + \mathbf{S}_{eh2} + \mathbf{S}_{eh2}^+}{2} \\ \Delta t \frac{\mathbf{P}_{he2} + \mathbf{S}_{he2} + \mathbf{S}_{he2}^+}{2} & \mathbf{T}_{hh2} \end{bmatrix} \begin{bmatrix} e_2^n \\ h_2^n \end{bmatrix} \\ + \begin{bmatrix} \Delta t \mathbf{S}_{eh21}^+ \\ \Delta t \mathbf{S}_{he21}^+ \end{bmatrix} \begin{bmatrix} e_1^{n+\frac{1}{2}} \\ h_1^{n+\frac{1}{2}} \end{bmatrix} + \begin{bmatrix} \Delta t \frac{\mathbf{S}_{eh2}^+}{2} \\ \Delta t \frac{\mathbf{S}_{he2}^+}{2} \end{bmatrix} \begin{bmatrix} e_2^{n+1} \\ h_2^{n+1} \end{bmatrix}. \quad (17)$$

The linear system of Eq. (17) will be solved iteratively and can be expressed as:

$$[\mathbf{T}] u_{i,k+1}^{n+1} = [\mathbf{S}_1] u_i^n + [\mathbf{S}_2] u_j^n + [\mathbf{S}_3] u_{j,k}^{n+1},$$

where subscript i represents the i th element, j represents the j th adjacent element, subscript k denotes the k th iteration. The initial value of $u_{j,0}^{n+1}$ in the right hand side of the equation is set to be the previous time step value u_j^n as $u_{j,0}^{n+1} = u_j^n$. After a few iterations for the solution of the $u_{i,k+1}^{n+1}$, the error can be acceptable and then go to the next step.

Iterative number for convergence determines the speedup effect of the method during the implementation. In this paper, the global iterative method is first proposed. By one-time iteration, all of the unknowns are obtained and compared with the results in the previous step. Root mean square error (RMSE) is calculated to determine whether the iteration is over or not. If the iteration is over, it will go to the next step. However, this method we first proposed with disadvantage of poor convergence performance will lead to increasing the iterative steps and enlarge the time step size. To solve this problem, a modified iterative CN method is further proposed. For this method, electromagnetic fields of each element are calculated by iteration and are updated immediately until all the elements are calculated and updated. Then RMSE is calculated. The procedure of the two proposed methods is given as Fig. 1 below.

Step 4. In region 1, CN scheme is employed in Eq. (6) and Eq. (7) to calculate the electric and magnetic fields at the time of $(n+1)\Delta t$:

$$\begin{cases} \mathbf{T}_{\text{ecl}} \cdot \frac{e_1^{n+1} - e_1^{n+\frac{1}{2}}}{\Delta t / 2} = \mathbf{P}_{\text{chl}} \cdot h_1^{n+\frac{1}{2}} + \mathbf{S}_{\text{chl}} \cdot h_1^{n+\frac{1}{2}} + \mathbf{S}_{\text{chl}}^+ \cdot h_1^{n+\frac{1}{2}} + \mathbf{S}_{\text{chl}2}^+ \cdot h_2^{n+1} \\ \mathbf{T}_{\text{hhl}} \cdot \frac{h_1^{n+1} - h_1^{n+\frac{1}{2}}}{\Delta t / 2} = \mathbf{P}_{\text{hel}} \cdot e_1^{n+1} + \mathbf{S}_{\text{hel}} \cdot e_1^{n+1} + \mathbf{S}_{\text{hel}} \cdot e_1^{n+1} + \mathbf{S}_{\text{hel}2}^+ \cdot e_2^{n+1} \end{cases}$$

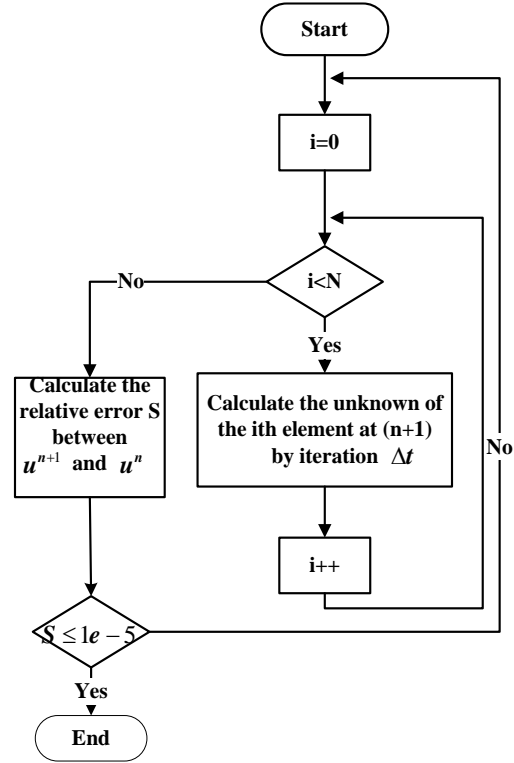
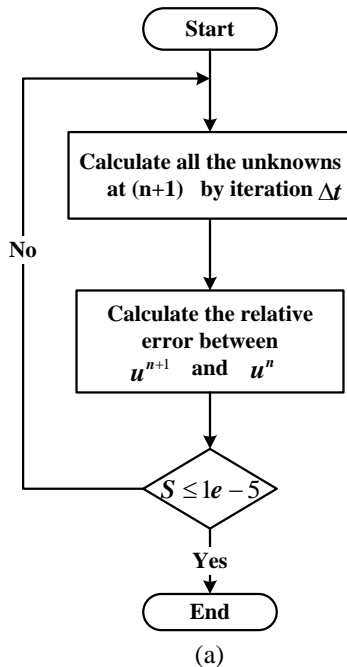


Fig. 1. (a) Flow chart of the iterative CN scheme, and (b) flow chart of the modified iterative CN scheme.

III. NUMERICAL RESULTS AND DISCUSSION

In order to verify the accuracy and efficiency of the proposed method, two numerical examples are analyzed. The first example is a rectangular cavity with the size of $10\text{mm} \times 5\text{mm} \times 15\text{mm}$. The number of the discretized tetrahedron is 1771 and the number of unknowns is 19015 and the time step size is 1.17×10^{-13} s which is five times as large as that of the leapfrog scheme. A modulated Gaussian pulse is selected as the excitation and the center frequency is 18GHz. The convergence speed is compared between iterative CN DG-FETD and modified iterative CN DG-FETD when both of the methods require 500 time steps. As shown in Fig. 2, the modified iterative CN DG-FETD can speed up the convergence effectively. The parameters of CN DG-FETD and iterative CN DG-FETD are also compared as shown in Table 1, which further demonstrates that the convergence speed of modified iterative CN method is superior to the iterative CN method and computational time of modified iterative CN method is much less than CN method.

The second example is a metal cylinder cavity loaded with a dielectric cylinder as shown in Fig. 3. The radius of the metal cylinder is 0.5m and the height is 1m. The radius of the dielectric cylinder is 0.05m, the

height is 0.02m and the relative permittivity is 4.0. A modulated Gaussian pulse is selected as the excitation in y direction with the center frequency of 230MHz. The number of the total discretized tetrahedron is 8464. The number of unknowns is 96089 with 14005 unknowns for the fine domain using CN method and 82084 unknowns for coarse domain using leapfrog method. The time step size is 1.33×10^{-11} s which is twice leapfrog time step size, Fig. 4 represents the transient scattering fields with two different method. Good agreement can be shown from the results obtained by the above different ways. Furthermore, Table 2 exhibits computational cost of the above different methods which further demonstrate the efficiency and accuracy of the proposed method.

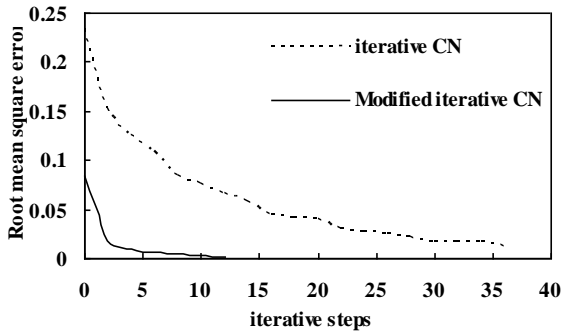


Fig. 2. Comparison of the convergence speed between two methods.

Table 1: Comparison of computational efficiency

Method	Number of Unknowns (CN)	Number of Unknowns (Leapfrog)	Iterative Steps	Iterative Time(s)
CN-leapfrog	14005	82084	5000	1104
Iterative CN-leapfrog	14005	82084	5000	650

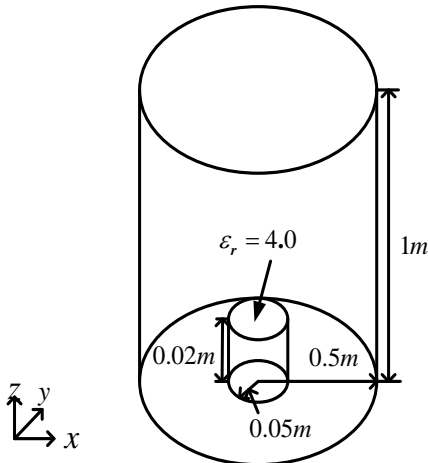


Fig. 3. A metal cylinder cavity loaded with a dielectric cylinder.

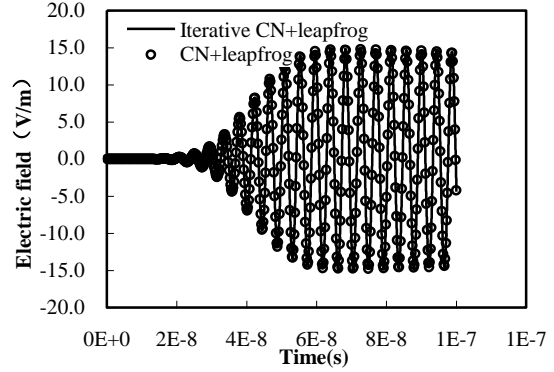


Fig. 4. Electric field in time domain calculated by the two methods.

Table 2: Comparison of computational efficiency

Iterative Method	Amplification of Time Step	Mean Convergence Step	Iterative Time(s)
CN	5	0	600
Iterative CN	5	35	415
Modified Iterative CN	5	13	173

IV. CONCLUSION

In the paper, a hybrid explicit-implicit iterative CN-leapfrog scheme based DG-FETD method is proposed for analysis of multiscale problems. The scheme divides the whole computational domain into two types. The iterative CN scheme is used in the fine regions while the leapfrog scheme is used in the coarse regions. Compared with the existing CN scheme and CN-leapfrog scheme, our scheme can not only enlarge the time step size but also ensure the mass matrix with the block diagonal characteristic. Numerical results show the accuracy and efficiency of the proposed iterative CN-leapfrog scheme DG-FETD.

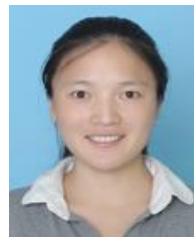
ACKNOWLEDGMENT

We would like to thank the support of the major project fund of natural science research in colleges and universities of Jiangsu province under grant No. 16KJA510003.

REFERENCES

- [1] T. Wan, R. S. Chen, and Z. D. Ding, "An efficient finite-element time-domain method via hierarchical matrix algorithm for electromagnetic simulation," *Appl. Comput. Electromag. Society J.*, vol. 26, no. 7, pp. 584-595, July 2011.
- [2] B. Cockburn, F. Li, and C. W. Shu, "Locally divergence-free discontinuous Galerkin methods for the Maxwell equations," *J. Comput. Phys.*, vol. 194, no. 2, pp. 588-610, Mar. 2004.

- [3] T. Lu, P. Zhang, and W. Cai, "Discontinuous Galerkin methods for dispersive and lossy Maxwell's equations and PML boundary conditions," *J. Comput. Phys.*, vol. 200, no. 2, pp. 549-580, Nov. 2004.
- [4] J. Chen and Q. H. Liu, "Discontinuous Galerkin time domain methods for multiscale electromagnetic simulations: A review," *Proc. IEEE*, vol. 101, no. 2, pp. 242-254, Feb. 2013.
- [5] S. D. Gedney, C. Luo, J. A. Roden, R. D. Crawford, B. Guernsey, J. A. Miller, T. Kramer, and E. W. Lucas, "The discontinuous Galerkin finite-element time-domain method solution of Maxwell's equations," *Appl. Comput. Electromag. Society J.*, vol. 24, no. 2, pp. 129-142, Apr. 2009.
- [6] S. Dosopoulos and J. F. Lee, "Interconnect and lumped elements modeling in interior penalty discontinuous Galerkin time-domain methods," *J. Comput. Phys.*, vol. 229, no. 2, pp. 8521-8536, Nov. 2010.
- [7] J. H. Lee, J. Chen, and Q. H. Liu, "A 3-D discontinuous spectral element time-domain method for Maxwell's equations," *IEEE Trans. Antennas Propag.*, vol. 57, no. 9, pp. 2666-2674, Sep. 2009.
- [8] S. Dosopoulos and J. F. Lee, "Interior penalty discontinuous Galerkin finite element method for the time-dependent first order Maxwell's equations," *IEEE Trans. Antennas Propag.*, vol. 58, no. 12, pp. 4085-4090, Dec. 2010.
- [9] S. Dosopoulos, B. Zhao, and J. F. Lee, "Non-conformal and parallel discontinuous Galerkin time domain method for Maxwell's equations: EM analysis of IC packages," *J. Comput. Phys.*, vol. 238, pp. 48-70, Dec. 2012.
- [10] S. Dosopoulos, J. D. Gardiner, and J. F. Lee, "An MPI/GPU parallelization of an interior penalty discontinuous Galerkin time domain method for Maxwell's equations," *Radio Science*, 46, pp. RSOM05, 2011.
- [11] C. Potratz, H.-W. Glock, and U. Van Rienen, "Time-domain field and scattering parameter computation in waveguide structures by GPU-accelerated discontinuous-Galerkin method," *IEEE Trans. Microw. Theory Tech.*, vol. 59, no. 11, pp. 2788-2797, Nov. 2011.
- [12] S. Gedney, C. Luo, B. Guernsey, J. A. Roden, R. Crawford, and J. A. Miller, "The discontinuous Galerkin finite-element time-domain method (DGFETD): A high order, globally-explicit method for parallel computation," *IEEE Int. Symp. on Electromagnetic Compatibility*, Honolulu, 2007.
- [13] R. Courant, K. Friedrichs, and H. Lewy, "On the partial difference equations of mathematical physics," *IBM J.*, vol. 11, no. 2, pp. 215-234, Mar. 1967.
- [14] V. Dolean, H. Fahs, L. Fezoui, and S. Lanteri, "Hybrid explicit-implicit time integration for grid-induced stiffness in a DGTD method for time domain electromagnetics," *Spectral and High Order Methods for Partial Differential Equations*, Berlin, Germany: Springer-Verlag, pp. 163-170, 2011, ser. Lecture Notes in Computational Science and Engineering.
- [15] H. Xu, D. Z. Ding, and R. S. Chen. "A hybrid explicit-implicit scheme for spectral-element time-domain analysis of multiscale simulation," *[J]. Journal of ACES*, vol. 31, no. 4, pp. 77-82, Apr. 2016.
- [16] J. M. Jin, *The Finite Element Method in Electromagnetics*. 2nd ed., New York: Wiley, 2002.



Min li received the M.S. degree in Electromagnetic Field and Microwave Technology from the School of Electrical Engineering and Optical Technique, Nanjing University of Science and Technology in 2012 and is currently working toward the Ph.D. degree in Nanjing University

of Posts and Telecommunications. Her research interests include semiconductor simulation, RF-integrated circuits and computational electromagnetics.



Xiaodong Ye was born in Jiangsu, China. He is currently an Associate Professor with the Electronic Engineering of NJUST. His current research interests include computational electromagnetics, electromagnetic scattering and radiation.